

Ground-based assessment of Total Ozone Mapping Spectrometer (TOMS) data for dust transport over the northeastern Mediterranean

Nilgün Kubilay, Temel Oguz, and Mustafa Koçak

Institute of Marine Sciences, Middle East Technical University, Erdemli, Turkey

Omar Torres

Joint Center for Earth Systems Technology, University of Maryland, Baltimore County, Baltimore, Maryland, USA

Received 16 September 2004; revised 11 January 2005; accepted 31 January 2005; published XX Month 2005.

[1] Multiyear daily surface aerosol aluminum (Al) concentration and sunphotometer measurements at Erdemli (Turkey) sampling station were used to assess the performance of Absorbing Aerosol Index (AAI) and Aerosol Optical Thickness (AOT) retrieved from the daily Total Ozone Mapping Spectrometer (TOMS) over the northeastern Mediterranean. A total of 98 moderate-to-high intensity dust events with durations from 1 day to 1 week were identified by aerosol Al concentrations and/or TOMS-AAI above their threshold values of $1.0 \mu\text{g m}^{-3}$ and 0.5, respectively. Only 15 events were found to bring appreciable dust load into the northeastern Mediterranean, predominantly below the 850-hPa pressure level, and therefore were not detected effectively by TOMS. Eight of these events corresponded to short-range high intensity intrusions ($\text{Al} > 3.0 \mu\text{g m}^{-3}$) from nearby dust sources of the Middle East and Arabian deserts, the rest (seven events) represented moderate-to-high intensity ($\text{Al} > 1.0 \mu\text{g m}^{-3}$) long-range transport from North Africa. Given the highly complex dynamics of the region, the use of TOMS-AAI data is justified for monitoring Saharan dust transport characteristics in the northeastern Mediterranean. Moreover, the TOMS-AOT data were found to covary linearly with its counterpart obtained by the ground-based measurements (correlation coefficient 0.86, significant at <0.001), which lies within the range of estimates suggested by earlier studies.

Citation: Kubilay, N., T. Oguz, M. Koçak, and O. Torres (2005), Ground-based assessment of Total Ozone Mapping Spectrometer (TOMS) data for dust transport over the northeastern Mediterranean, *Global Biogeochem. Cycles*, 19, XXXXXX, doi:10.1029/2004GB002370.

1. Introduction

[2] Being highly oligotrophic and limited with nutrient supply from rivers, atmospheric deposition in general and Saharan-based mineral dust in particular constitute an essential component of the biogeochemical cycle in the Mediterranean Sea. The Aeolian input of nutrients (phosphate and iron) acts as the most effective external source for promoting enhanced biological production locally and episodically in the sea [Krom *et al.*, 2004]. The measurements in the western basin [Guieu *et al.*, 2002a, 2002b] indicated that the contributions of phosphorus and iron from the Saharan dust account for ~ 30 – 40% and $\sim 96\%$ of their total atmospheric fluxes, respectively. Although the impact of Saharan dissolved inorganic phosphate for the new production at basin and annual scales may not be significant, its contribution on event timescale represents an important part of the integrated new production, as indicated by measurements in the western

Mediterranean [Ridame and Guieu, 2002], in the central Mediterranean (Crete) and the eastern Mediterranean (Erdemli) [Markaki *et al.*, 2003] during stratified (summer-autumn) periods. Estimation of dust associated atmospheric nutrient fluxes indirectly by means of remote-sensing-derived products is an area of growing interest because of their capability of providing continuous time series data at different spatial resolutions.

[3] Total Ozone Mapping Spectrometer (TOMS)-Absorbing Aerosol Index (AAI) constitutes one of the most useful space-borne data sets, offering long-term daily and global information on UV absorbing aerosol (black carbon, desert dust) distributions [Herman *et al.*, 1997; Torres *et al.*, 1998]. A compilation of nearly 2 decades of data has already provided a more precise identification of tropospheric aerosol characteristics surrounding distinct source areas [e.g., σ , 2002; Prospero *et al.*, 2002; Washington *et al.*, 2003], and long-range transport over continents and oceans [e.g., Hsu *et al.*, 1999; Chiapello *et al.*, 1999; Chiapello and Moulin, 2002; Moulin and Chiapello, 2004]. It is therefore regarded as one of the potential sources for monitoring the dust transport characteristics in the

72 Mediterranean region as well. In addition to the TOMS
73 AAI, an aerosol optical depth product derived from TOMS
74 observations is also available.

75 [4] TOMS-AAI data were used for the North Africa and
76 Mediterranean regions by *Israelevich et al.* [2002] for
77 identifying distinct North African desert dust aerosol sour-
78 ces, the way in which dust was transported eastward and
79 northward, and the way it varied on a daily basis over the
80 eastern (25°E–35°E), central (12°E–22°E), and western
81 (0°–10°E) basins of the Mediterranean Sea. Apart from
82 this work, only a few studies have dealt with the satellite-
83 based characterization of dust transport over the Mediterra-
84 nean. *Moulin et al.* [1998] presented the seasonal climatol-
85 ogy of North African dust transport over the Mediterranean
86 basin using dust optical thickness data for June 1983
87 through December 1994, retrieved from the daily visible
88 radiances measured by Meteosat. A similar seasonal dust
89 optical thickness variation over the Mediterranean was also
90 obtained from MODIS data for the year 2001 by *Barnaba*
91 *and Gobbi* [2004]. Using visible radiances from AVHRR on
92 the NOAA-9 and NOAA-11 satellites over a 1-year period
93 (August 1988 to September 1999), *Dayan et al.* [1991]
94 examined some specific dust intrusion events in the central
95 and eastern Mediterranean, and identified preferentially
96 high or low altitude transports from two distinct sources:
97 the Sahara and the Middle East-Arabian Desert. *Kubilay*
98 *and Saydam* [1995] and *Kubilay et al.* [2000, 2003] noted
99 individual contributions of these sources, together with
100 distinctly different chemical and physical properties, to
101 mineral dust loading in the northeastern Mediterranean
102 atmosphere.

103 [5] So far, *Chiapello et al.* [1999] provided the only long-
104 term independent data sets used for validating the temporal
105 record of the TOMS-AAI. They documented the mineral
106 dust transport characteristics across the North Atlantic by
107 measuring ground-based mineral dust concentrations at four
108 sampling stations (Sal Island, Tenerife, Barbados, and
109 Miami). These measurements indicated that TOMS was
110 able to detect 99% of the events recorded by surface dust
111 concentration measurements at Tenerife station located at an
112 altitude of 2400 m, well above the boundary layer and in a
113 region of the troposphere where Saharan dust is usually
114 transported. In contrast, monthly variations of the TOMS-
115 AAI and surface mineral dust concentrations were shown to
116 differ significantly at Sal Island. In winter, when dust was
117 transported at low altitudes in the trade wind layer, surface
118 measurements indicated high dust concentrations in contrast
119 to threshold TOMS-AAI values of around 0.5. In summer,
120 when dust transport switched to high altitude mode, the
121 TOMS-AAI values attained a maximum (around 2–3),
122 whereas surface dust concentrations decreased to their
123 lowest levels. Surface measurements carried out at Barba-
124 dos and Miami showed some capability for the TOMS-AAI
125 in detecting high altitude African mineral dust transport
126 events over the North Atlantic Ocean. Good agreement
127 between the TOMS-AAI and surface dust concentrations
128 was found over Israel for a strong dust storm event during
129 14–17 March 1998 [*Alpert and Ganor*, 2001].

130 [6] Our long-term (1991–1992, 1996–2002) daily
131 surface aerosol aluminum (Al) concentration measurements

performed at the Erdemli sampling site constitute yet 132
another valuable independent data set for assessing the 133
performance of the TOMS-AAI in the northeastern 134
Mediterranean, and for exploring regional dust transport 135
characteristics (e.g., frequency, direction, thickness, inten- 136
sity of high and low altitude transports). Highly dynamic 137
intrusions from different nearby sources (the Sahara in the 138
south-southwest, the Middle East-Arabian Desert in the 139
east-southeast, and Anatolia and the Balkans in the north- 140
northwest) with a complex vertical structure [*Dayan et al.*, 141
1991; *Hamonou et al.*, 1999; *Kubilay et al.*, 2000, 2003; 142
Alpert et al., 2004] makes the northeastern Mediterranean 143
an ideal test site for assessing the performance of TOMS 144
products. In the present study, we first make use of all 145
available TOMS-AAI data over the northeastern Mediterra- 146
nean to point out the frequency, intensity, and seasonal 147
patterns of specific intrusion events. The assessment of the 148
use of the TOMS-AAI for detecting mineral dust aerosol 149
content exported from different sources around our analysis 150
region is then provided by means of daily aerosol Al 151
concentration measurements. Finally, the TOMS Aerosol 152
Optical Thickness (AOT) data are compared with the AOT 153
data derived from the ground-based Sun photometer mea- 154
surements to assess the performance of the AOT retrieval 155
directly from the TOMS for northeastern Mediterranean 156
conditions. 157

2. Data Description 158

[7] The 21-year-long (1979–1992 and 1996–2002) 159
record of Absorbing Aerosol Index (TOMS-AAI) data were 160
obtained from observations by the TOMS/Nimbus-7 161
(1979–1992) and TOMS/Earth Probe (1996–2002) sen- 162
sors. The TOMS AAI is a very useful qualitative parameter 163
for the detection of the presence in the atmosphere of UV- 164
absorbing aerosols, and for the identification and analysis of 165
dust and smoke transport patterns. Because of its qualitative 166
nature, the TOMS-AAI is sensitive to absorbing aerosols 167
even when mixed with clouds. The AAI data is available on 168
a daily basis, on a 1° (latitude) by 1.25° (longitude) 169
resolution. Positive TOMS-AAI values around our sampling 170
station at Erdemli (see Figure 1 for its location) were 171
obtained as an average of nine pixels in the small box 172
confined by 33.0°E–35.5°E and 35.5°N–37.5°N. 173

[8] Aerosol data from TOMS observations is also avail- 174
able as AOT, obtained from a retrieval algorithm [*Torres et* 175
al., 1998, 2002], that uses as input the measured radiances 176
at two near UV wavelengths (331 and 360 nm for the 177
EP-TOMS sensor). The derived quantities are optical depth 178
and single scattering albedo (SSA). Unlike the AAI, which 179
is mainly sensitive to UV-absorbing aerosols, the TOMS 180
near UV retrieval algorithm are sensitive to all aerosol types 181
regardless of their altitude and absorption properties. Vali- 182
dation analysis of both the AOT [*Torres et al.*, 2002, 2005] 183
and single scattering albedo [*Torres et al.*, 2005] using 184
AERONET measurements, show that in general, the TOMS 185
AOT retrievals are within 30% of the AERONET observa- 186
tions for absorbing aerosols and 20% for non-absorbing 187
aerosols. The TOMS retrieved AOT and SSA are affected 188
by cloud contamination, and, therefore, their temporal and 189

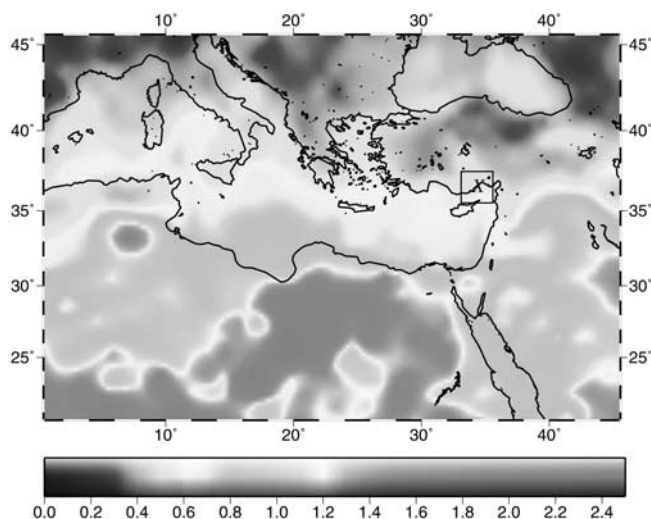


Figure 1. April-mean TOMS-AAI distribution obtained by averaging 21 years of daily data at each pixel of the analysis region. Three distinct regions with different TOMS-AAI properties are clearly indicated in the map. North Africa (red) identifies the major dust load (TOMS-AAI ≥ 1.0), whereas Southern Europe and Asia Minor (blue) (TOMS-AAI ≤ 0.4) represent a negligible dust load. The eastern Mediterranean is a transitional region with latitudinal TOMS-AAI variations between 1.0 in the south and 0.5 in the north. The Erdemli sampling station, as well as a small box around it, near the northeastern corner of the eastern Mediterranean is also shown in the figure. See color version of this figure at back of this issue.

190 spatial coverage are not as large as the coverage provided by
191 the AAI.

192 [9] Ground-based aerosol sampling and analysis at the
193 Erdemli coastal station were carried out during the periods
194 of August 1991 through December 1992, January 1996
195 through May 1997, February 1998 through May 2000, and
196 January 2001 through December 2002. Apart from some
197 seasonal gaps in the data during the study period, measure-
198 ments have sampling interruptions of a few days to a week
199 every month due to the malfunctioning of sampling instru-
200 ment. The sampling and analytical procedures together with
201 some findings from these measurements were reported by
202 *Kubilay and Saydam* [1995], *Kubilay et al.* [2000], and
203 *Koçak et al.* [2004].

204 [10] As a part of the ground based Aerosol Robotic
205 Network (AERONET) Program, the columnar integrated
206 aerosol optical properties (e.g., aerosol optical thickness,
207 single scattering albedo, Ångström coefficient, and refrac-
208 tive index) were retrieved daily at the Erdemli coastal
209 station during the 1.5-year period from January 2000
210 through June 2001 as a product of direct sun radiance
211 measurements by the CIMEL Sun photometer/sky radiom-
212 eter [*Kubilay et al.*, 2003].

213 [11] Transport routes of air masses ending at our sampling
214 site at 1000-, 850-, 700-, and 500-hPa pressure levels were
215 determined by the three-dimensional, 3-day air mass back
216 trajectory analysis using wind fields provided by the

European Centre for Medium-Range Weather Forecasts 217
(ECMWF). 218

[12] Daily TOMS-AAI values corresponded to instanta- 219
neous satellite measurements made during the overpass once 220
a day at about 1130 local time, whereas the daily aerosol AI 221
concentrations were obtained by continuous sampling over a 222
nominal 24-hour period. Similarly, the values of aerosol 223
optical properties were based on the daily averaging of the 224
measurements repeated every 15 min. Considering the fact 225
that the dust concentrations may have a strong daily cycle 226
[*Alpert and Ganor*, 2001] and satellite overpass time does 227
not necessarily coincide with the time of typical dust 228
loading, TOMS-AAI values thus may not truly represent 229
the daily mean conditions as compared to the other two data 230
sets. Reliability of once-a-day TOMS-AAI measurements is 231
further hampered by cloudiness. The ground-based mea- 232
surements include contribution of all aerosols, whereas the 233
TOMS-AAI specifically represents the contribution by 234
absorbing aerosols. These differences may introduce some 235
difficulties and uncertainties in their comparisons. 236

3. Mineral Dust Over the Northeastern 237 Mediterranean 238

3.1. Spatial Distribution of the TOMS-AAI 239

[13] The long-term mean April TOMS-AAI distributions 240
computed by averaging 21 years of the daily data for 241
UV-absorbing aerosols at each pixel of the region 242
surrounded by 20.5°N and 45.5°N latitudes and 0.0° and 243
45.5°E longitudes is shown in Figure 1. April was specifi- 244
cally chosen since dust transports are particularly intensi- 245
fied over the eastern Mediterranean (hereinafter also 246
referred to as EMed) atmosphere during this period 247
(Figure 2) [see also *Ganor*, 1994; *Moulin et al.*, 1998; 248
Israelevich et al., 2002]. In general, the TOMS-AAI distri- 249
bution reveals considerable latitudinal variations from the 250
most intense dust load in the south to a negligible load over 251
the continental landmass in the north. North Africa is 252
characterized by highest dust accumulation with TOMS- 253
AAI > 1.0 . The red spot with TOMS-AAI ~ 2.0 over the 254
Eastern Sahara has been identified as “source region D” 255
(centered at $\sim 25^\circ\text{N}$, 18°E) by *Israelevich et al.* [2002], and 256
forms the northward extension of the Sahel to the south of 257
20°N. The red spot on the eastern end of the region 258
represents either a local dust source over the Saudi Arabian 259
Desert or eastward transport from the Sahara. 260

[14] The EMed atmosphere yields latitudinal TOMS-AAI 261
variations between 1.0 and 0.6. This long-term mean dust 262
distribution is, however, known to be modified by episodic 263
dust intrusions, specific examples of which were provided 264
earlier by *Kubilay and Saydam* [1995], *Özsoy et al.* [2001], 265
Alpert and Ganor [2001], *Israelevich et al.* [2002], *Kubilay* 266
et al. [2000; 2003], and *Koçak et al.* [2004]. The western 267
Mediterranean atmosphere is, on the other hand, less 268
affected by dust transports during this period. As reported 269
by *Moulin et al.* [1998], *Israelevich et al.* [2002], and 270
Barnaba and Gobbi [2004], the western basin receives the 271
maximum dust transport in summer months. When long- 272
term mean monthly data are taken into account, as shown in 273
Figure 1, both North African and Middle East dust sources, 274

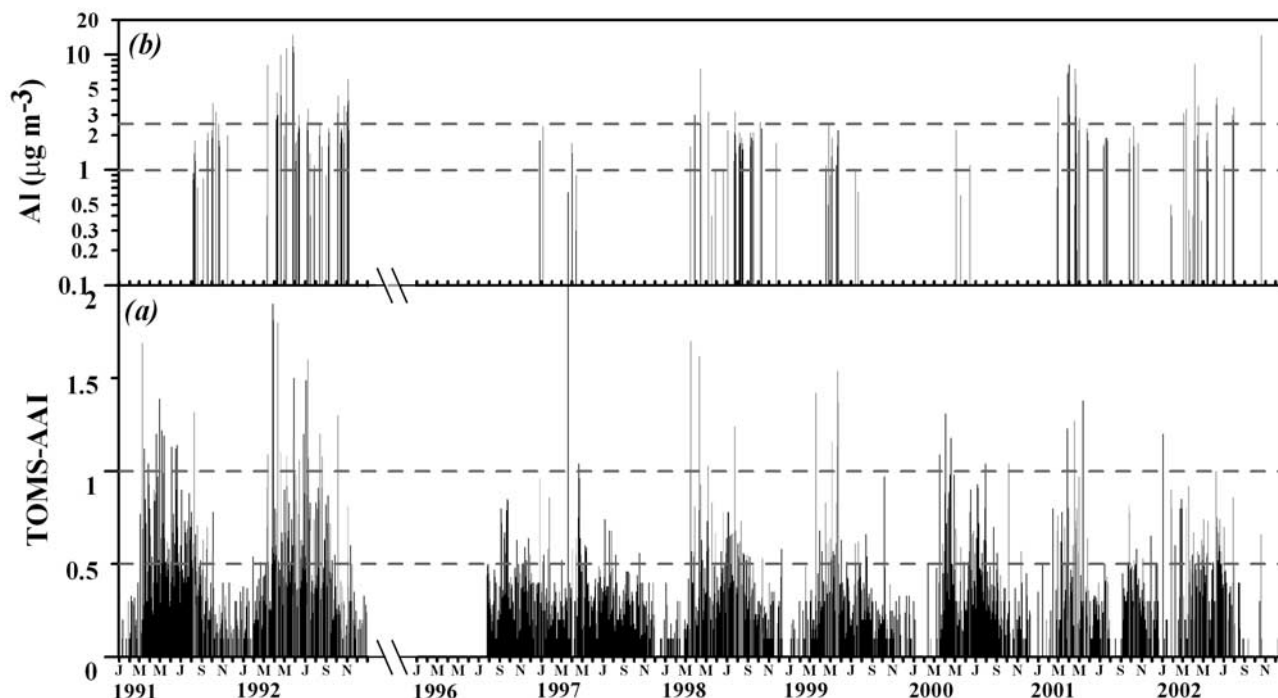


Figure 2. (a) Daily TOMS-AAI distribution around Erdemli during 9-year period from 1 January 1991 to 31 December 1992 and 26 July 1996 to 31 December 2002 (black bars). Superimposed on this data, red bars indicate dust events either with TOMS-AAI > 0.5 or aerosol AI > 1.0 or both, for common days with TOMS-AAI and aerosol AI data. Two broken horizontal lines represent the threshold AAI values for moderate and intense dust events classified on the basis of TOMS retrievals. (b) Daily aerosol AI ($\mu\text{g m}^{-3}$) measurements performed during the study period. The data represent a subset of all the available measurements corresponding to the events shown by red bars in Figure 2a. Two broken horizontal lines indicate the threshold values for moderate and intense dust events classified according to the ground-based measurements. See color version of this figure at back of this issue.

275 however, have limited intrusions over Anatolia and South-
 276 ern Europe. TOMS-AAI values less than 0.5 for these
 277 regions are therefore considered to represent the background
 278 state with negligible spring dust transport.

280 3.2. Interannual Variations of the TOMS-AAI

281 [15] Figure 2a shows daily TOMS-AAI values within the
 282 box around our sampling station at Erdemli. Only the
 283 periods of 1991–1992 and 1996–2002, which are common
 284 with surface aerosol AI measurements, are given in this plot;
 285 other years possess similar features except for some year-
 286 to-year variations in terms of intensity and timing of events.
 287 Within the study period under consideration here, a total of
 288 1070 common daily data pairs of the TOMS-AAI and
 289 surface aerosol AI concentrations were available at Erdemli.
 290 Only 225 of the events corresponded to dusty days, which
 291 are defined either by aerosol AI concentrations greater than
 292 $1.0 \mu\text{g m}^{-3}$ (Figure 2b) or by AAI values greater than 0.5
 293 (shown in Figure 2a by red color), or both. These dust
 294 events with transports from the Sahara or the Middle East
 295 were further supported by the air mass back trajectory
 296 analysis. The rest, with values below the thresholds, repre-
 297 sent the no-dust and/or negligible dust transport cases.

298 [16] Following *Herman et al.* [1997] and *Chiapello et al.*
 299 [1999], TOMS-AAI = 0.5 is chosen here as the threshold for

TOMS detection of absorbing aerosols, even though any 300
 choice between 0.3 and 0.6 seems to be acceptable. Looking 301
 at the data in Figure 2a, this value may be considered a 302
 rather conservative choice for monitoring dust. In order to 303
 simplify the analysis, the dust transports inferred from the 304
 TOMS were classified as either “moderate intensity” for 305
 AAI values between 0.5 and 1.0 or “high intensity” for 306
 AAI ≥ 1.0 . The latter threshold value was chosen somewhat 307
 arbitrarily on the basis of the data given in Figure 2a. 308
 Similar distinction was also adopted for identifying trans- 309
 ports by the aerosol AI data. Following *Kubilay et al.* 310
 [2000], the moderate intensity events were classified by 311
 concentrations between $1.0 \mu\text{g m}^{-3}$ and $2.5 \mu\text{g m}^{-3}$, and 312
 high intensity events by $\text{AI} \geq 2.5 \mu\text{g m}^{-3}$. These boundaries 313
 were shown in Figures 2a and 2b by broken lines. There 314
 was, however, no particular reason for the choices of these 315
 thresholds except an overall assessment of the whole data 316
 set, and different values may in fact be assigned for other 317
 regions depending on local dust transport characteristics. 318

[17] The data shown in Figure 2a indicate a regular 319
 pattern of seasonal variations characterized by a lack of 320
 appreciable dust intrusions during the late autumn-winter 321
 months from November to the middle of March, and 322
 episodic enhanced dust outbreaks during the rest of the 323
 year. The most intensive events take place in the second half 324

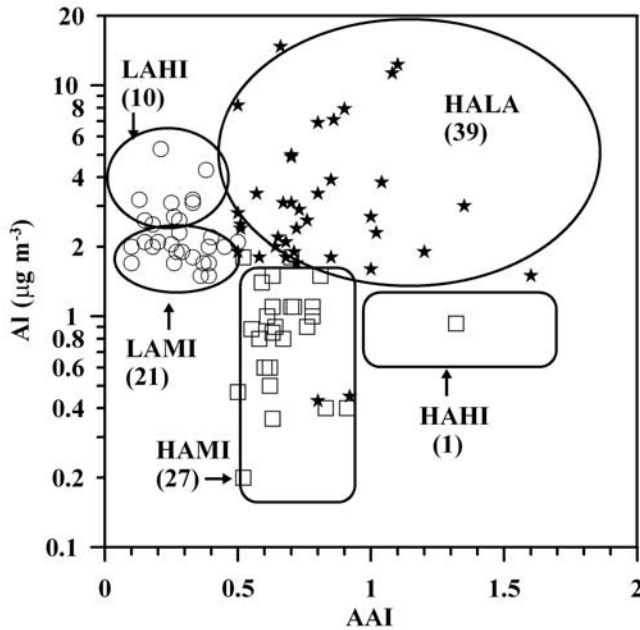


Figure 3. Scatterplot of aerosol Al concentrations and the corresponding TOMS-AAI values for the total of 98 events presented in Figure 2. HAMI and HAHI refer to “High Altitude Moderate Intensity” and “High Altitude High Intensity” modes, respectively, of dust transport. Similarly, LAMI and LAHI refer to “Low Altitude Moderate Intensity” and “Low Altitude High Intensity” modes, respectively. HALA mode denotes the dust events transported at both “High Altitude and Low Altitude”. The numbers in parentheses show the number of total dust events for each particular mode.

of March, April, and May as also suggested previously by the dust optical thickness data [Moulin *et al.*, 1998; Barnaba and Gobbi, 2004], the TOMS-AAI data [Israelevich *et al.*, 2002], and the Sun photometer data [Kubilay *et al.*, 2003], as well as the ground-based aerosol measurements [Kubilay *et al.*, 2000]. Relatively strong dust intrusion events are also observed occasionally during the autumn until early November. The year 2002 was exceptional in terms of major dust transport period, which shifted earlier to January–March. These intrusions are characterized in our analysis region by $0.5 < \text{TOMS-AAI} < 1.0$, indicating moderately intense dust loads. Their frequency is approximately 18% of the entire data set. More intense dust loads ($\text{TOMS-AAI} > 1.0$) are also noticeable in the data set. They constitute 3% of the entire data set, corresponding to six to eight events per year during the early 1990s, and decrease to one to three events per year toward the end of the 1990s and the early 2000s. The years 1996 and 1997 were particularly poor in terms of dust loading into the northeastern Mediterranean, even for moderate intensities. The decreased dust transport activity inside the Mediterranean basin during these years has been related to the North Atlantic Oscillation by Moulin *et al.* [1997]. The rest of the data set with $\text{TOMS-AAI} \leq 0.5$ implies background conditions, without any dust transport signature. The entire late autumn-winter

period as well as a part of summer season generally falls into this category, with a few exceptions.

3.3. Assessment of the TOMS-AAI

[18] Two-hundred-twenty-five days of the common data set of the dusty days shown in Figure 2 characterize 98 specific dust events with periods varying from 1 day to 1 week, but most commonly 2–3 days. If events lasted longer than 1 day, representative values of the TOMS-AAI and aerosol Al concentrations for each event were obtained by averaging their values over the duration of the event. The events are characterized by a wide range of aerosol Al concentrations and TOMS-AAI values: up to $15 \mu\text{g m}^{-3}$ for the former, and 1.6 for the latter. The “low altitude” transport to the analysis region is traced by the air mass back trajectories arriving at 1000- and 850-hPa pressure levels, and quantified by surface aerosol Al concentrations. The “high altitude” transport traced by air mass back trajectories arriving at the 700- and 500-hPa pressure levels, and intensity is quantified by the TOMS-AAI values. As mentioned in the preceding section, both high and low level transports were classified as either “moderate intensity” or “high intensity” according to pre-assigned threshold values of the aerosol Al concentration and TOMS-AAI. These modes of dust events over the northeastern Mediterranean are shown in Figure 3 by the scatterplot of the TOMS-AAI values versus aerosol Al concentrations.

[19] All together, 67 events involved high level transport (i.e., $\text{TOMS-AAI} > 0.5$). Their air mass back trajectories and the corresponding vertical motions during the last 3 days of their excursion (Figures 4a and 4b) suggest that an overwhelming proportion of the transport originated from the Sahara and at different altitudes. While most of the transports cross the EMed at preferentially high altitudes, some of them first start their excursion at lower levels and then rise toward higher levels on their way to the analysis region. In fact, 28 of these events attain no additional low level transport (since $\text{Al} < 1.0 \mu\text{g m}^{-3}$) and are considered to be confined to the levels above the 850-hPa pressure level. These are shown in Figure 3 by the high altitude–moderate intensity (HAMI), and the high altitude–high intensity (HAHI) modes. Thirty-nine of them are also accompanied with low level transport (since $\text{Al} \geq 1.0 \mu\text{g m}^{-3}$) and therefore represent a vertically thicker and homogenous dust column (denoted by High Altitude Low Altitude, HALA mode in Figure 3).

[20] As documented in Table 1, 64 of the high level transports are directed from the south-southwest (S-SW), originating from the central and eastern Sahara, two from the north-northwest (N-NW) over western Anatolia and Balkans, and only one case from the southeast, Arabian Desert. Thus 96% of the events involve the long-range excursion of dust from the Sahara above 850 hPa. Moreover, 57 of these high altitude transports are classified as moderate intensity events with a mean AAI value of 0.68. The remaining 10 characterize high intensity events generally taking place in the spring months, with a mean AAI value of 1.17 (Table 1). As demonstrated by Kubilay *et al.* [2000] for selected events from 1992, and also described by Moulin *et al.* [1998] and Israelevich *et al.* [2002], these high

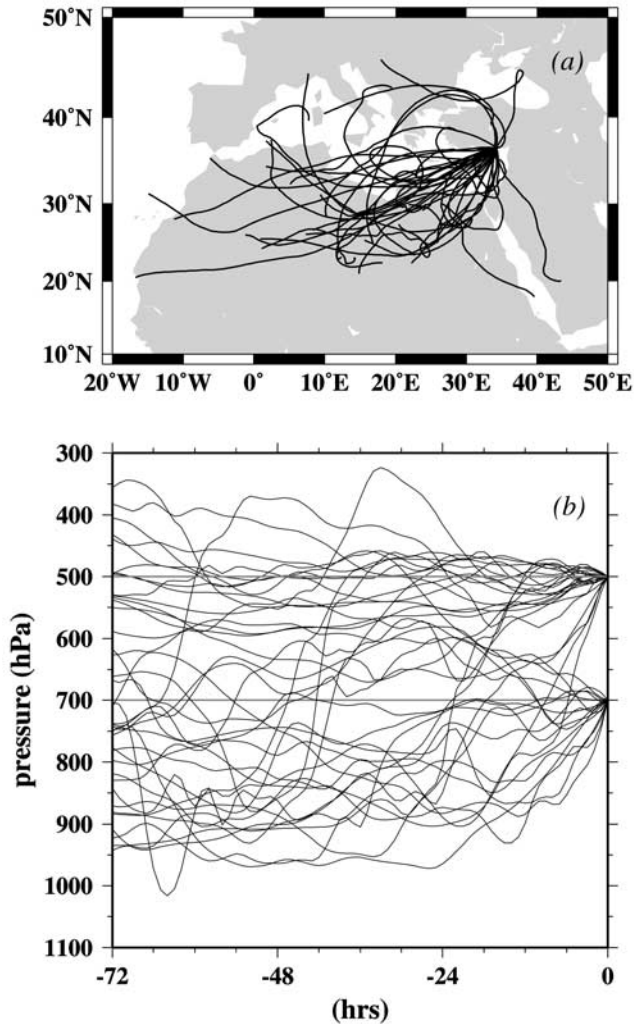


Figure 4. (a) Three-day back trajectories for high altitude transport events arriving at 700- and 500-hPa pressure levels to Erdemli, and (b) their vertical motions along the trajectories. They represent some selected events out of a total 67 during 1991–1992 and 1996–2002. See color version of this figure at back of this issue.

intensity spring events are generally products of dust storms associated with developing cyclones over the Sahara. As they form, these intense cyclones uplift substantial amounts of dust from the surface, ascend to higher altitudes by strong upward motion, and subsequently export dust to the northeastern Mediterranean as they travel toward the east-northeast (see *Alpert and Ganor* [2001] for a specific case study). The remaining moderate intensity high level transports are suggested to be generally driven by mobilization of a dust load already accumulated at high altitudes of the atmosphere above North Africa in the spring-summer months by appropriate synoptic systems. As shown quantitatively by *Israelevich et al.* [2002], the flux of dust from sources in North Africa exceeds sinks due to the low settling and transport in spring and summer. As a result, the atmosphere over Northern Africa is almost permanently loaded with significant amounts of mineral desert dust. The major

portion is exported over the North Atlantic [e.g., *Hsu et al.*, 1999; *Chiapello et al.*, 1999; *Chiapello and Moulin*, 2002; *Moulin and Chiapello*, 2004], but some moves northward over the eastern Mediterranean.

[21] The remaining 31 events are confined to the boundary layer (below 850 hPa) without any high altitude contribution when they arrive in the northeastern Mediterranean (Figure 5a). They correspond to low altitude–moderate intensity (LAMI) and low altitude–high intensity (LAHI) modes in Figure 3. They constitute $\sim 30\%$ of the total events not captured by TOMS, as evident by the TMS-AAI values of around 0.3 in our analysis region. A closer inspection of these low level only transport events suggests that 24 of them come from sources in close proximity of our analysis region, 16 from Anatolia (N-NW) with moderate aerosol AI concentrations of $1\text{--}2\ \mu\text{g m}^{-3}$ implying no appreciable dust input into the region, and eight from the Middle East (E-SE) with aerosol AI concentrations greater than $3\ \mu\text{g m}^{-3}$ (Table 2). These sources are very close to our analysis region for the establishment of the long-range, high altitude transports, and thus TOMS is unable to capture them. The remaining seven “low level” dust events represent high intensity long-range transport from the Sahara (S-SW) (see Figure 5b) with AI concentrations about $2\text{--}5\ \mu\text{g m}^{-3}$. Consequently, as far as long-range dust transport originated from North Africa is concerned, TOMS is unable to capture only seven events out of a total of 98. The use of TOMS-AAI data for monitoring Saharan dust transport characteristics in the northeastern Mediterranean is therefore justified, given its highly complex dynamic structure.

3.4. Comparison of TOMS and AERONET Optical Depth

[22] The quantitative use of the AAI as an indicator of aerosol amount is hampered by the multiple dependencies of the AAI on aerosol optical depth, elevation of the aerosol layer above the ground, absorption properties, and particle size distribution as documented in the literature [*Torres et al.*, 1998; *Herman et al.*, 1997]. Thus a more quantitative evaluation of the TOMS aerosol measurements can be carried out using the AOT product described in section 2.

[23] Using the TOMS-AOT orbital data averaged over a $2^\circ \times 2^\circ$ box centered at our site Erdemli (converted to 440 nm), the TOMS retrievals of aerosol optical thickness were compared to the ground-based AERONET observa-

Table 1. Summary Statistics of Total High Level Dust Transport Events With or Without the Accompanying Low Level Transports^a

	Number of Events	Duration	AAI	AI, $\mu\text{g m}^{-3}$
		<i>Intensity</i>		
Moderate	57	130	0.68	2.33
High	10	22	1.17	1.13
		<i>Direction</i>		
S-SW	64	148	0.75	2.63
E-SE	1	2	0.70	4.9
N-NW	2	2	0.85	0.75

^aEvents are expressed in terms of intensity and direction, total duration, and mean values of the TMS-AAI and aerosol AI concentrations.

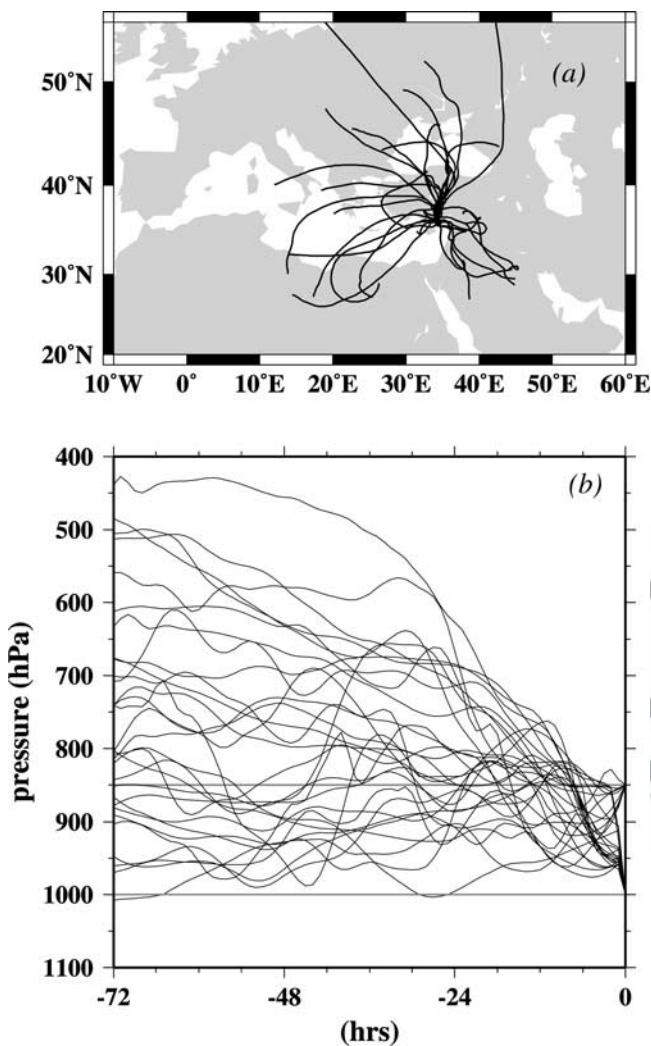


Figure 5. (a) Three-day back trajectories for low altitude transport events arriving at 1000- and 850-hPa pressure levels to Erdemli, and (b) their vertical motions along the trajectories. They represent some selected events out of a total 31 during 1991–1992 and 1996–2002. See color version of this figure at back of this issue.

472 tions for the period of January 2000 to June 2001. When all
473 the AERONET data (a total of 116 measurements) were
474 included, the scatterplot in Figure 6 depicts a linear fit
475 (given by the thick continuous line) with the correlation
476 coefficient 0.87 (significant at $p < 0.001$). The TOMS
477 retrievals are found to account for 79% of the ground-based
478 measurements. This level of agreement lies within the 30%
479 range of theoretically predicted uncertainty [Torres *et al.*,
480 2002].

481 [24] As shown by Kubilay *et al.* [2003], a sharp drop in
482 the Angström coefficient to values near zero is among the
483 most prominent features of dust episodes observed in the
484 northeastern Mediterranean. Thus, when a subset of
485 the AERONET data (41 measurements) was used represent-
486 ing specifically dust aerosols with the Angström coefficient
487 values less than 1.0, the agreement between the TOMS and

Table 2. Summary Statistics of Low Level Transport Events Only, Without the Accompanying High Level Transports^a

	Number of Events	Duration	AAI	AI, $\mu\text{g m}^{-3}$	
		<i>Intensity</i>			t2.3
Moderate	21	57	0.31	1.9	t2.4
High	10	17	0.29	3.3	t2.5
		<i>Direction</i>			t2.7
S-SW	7	19	0.23	2.9	t2.8
E-SE	8	14	0.29	2.8	t2.9
N-NW	16	41	0.34	1.9	t2.10

^aEvents expressed in terms of intensity and direction, total duration, and mean values of the TOMS-AAI and aerosol AI concentrations.

t2.11

AERONET measurements of AOT increases to 86% with
488 the correlation 0.91 (see broken line in Figure 6). The
489 difference between the AOT values of the TOMS and
490 AERONET data sets is thus smaller, indicating a rather
491 successful estimation of the AOT from TOMS for
492 the northeastern Mediterranean. The difference can be
493 explained by a combination of various factors such as
494 sensitivity of the TOMS algorithm to the altitude of the
495 mineral dust layer and sub-pixel cloud contamination,
496 aerosol composition and size distribution, and sampling
497

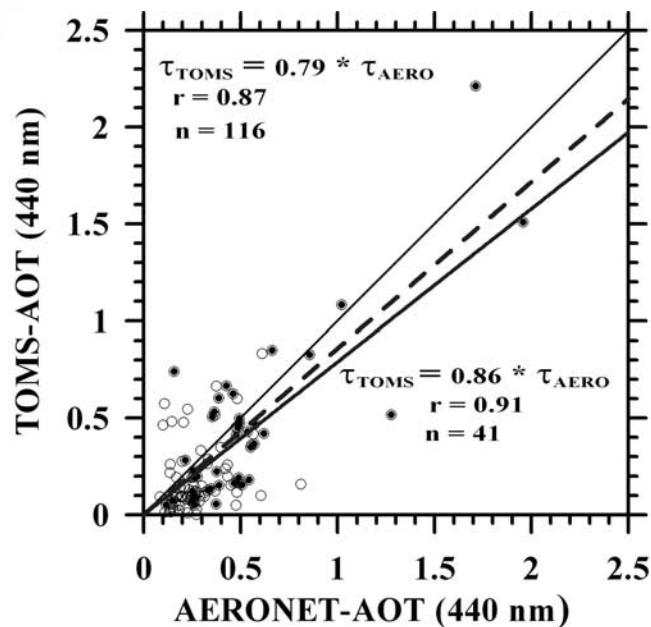


Figure 6. Scatterplot of TOMS-AOT versus AERONET-AOT at 440 nm for the northeastern Mediterranean during January 2000 to June 2001. The thin continuous line represents one-to-one line. The thick continuous line depicts the linear regression when all the available AERONET measurements ($n = 116$, open circles) are included. In this case, the data sets are related to each other linearly by $\tau_{\text{TOMS}} = 0.79 \tau_{\text{AERONET}}$. The dashed line denotes the linear regression when a subset of the AERONET data ($n = 41$, solid circles) representing only the mineral dust cases with Angström coefficient less than 1.0. Then, the data sets covary with the relation $\tau_{\text{TOMS}} = 0.86 \tau_{\text{AERONET}}$.

498 frequency (daily for the sunphotometer versus instantaneous
499 for TOMS).

501 4. Conclusions

502 [25] In the present study, the 21-year-long (1979–1992
503 and 1996–2002) daily Total Ozone Mapping Spectrometer
504 Absorbing Aerosol Index (TOMS-AAI) and the multiyear
505 (1991–1992, 1996–2002) daily surface aerosol aluminum
506 (Al) concentration measurements at Erdemli sampling station
507 were used to assess the capability of the TOMS-AAI in
508 detecting mineral dust over the northeastern Mediterranean,
509 when they are exported from North Africa and/or the
510 Middle East.

511 [26] When all available common daily surface aerosol Al
512 and TOMS-AAI measurements were taken into consideration
513 (1070 data pairs in all), 98 specific dust events were
514 identified for the northeastern Mediterranean. Seventy per-
515 cent (67 events) involved moderate-to-intense high altitude
516 transport. They were further accompanied with varying
517 contributions of low level transport characterized by a wide
518 range of surface aerosol Al concentrations, and mostly
519 originated from the Sahara. The remaining 30% (31 events),
520 on the other hand, predominantly took place below 850-hPa
521 level, and were not detected effectively by TOMS. Sixteen
522 of these low altitude events represented short-range dust
523 intrusions from Anatolia and the Balkans in the north-
524 northwest. They were weak-to-moderate intensity events,
525 and therefore unable to introduce appreciable dust loads into
526 the northeastern Mediterranean. Eight of the remaining 15
527 events corresponded to short-range high intensity intrusions
528 from nearby dust sources of the Middle East, while the other
529 seven events were ascribed to long-range transport from
530 North Africa, undetected by TOMS. Given the highly
531 complex dynamics of the region, the use of TOMS-AAI
532 data is therefore justified for monitoring Saharan dust
533 transport characteristics in the northeastern Mediterranean.
534 Within the entire 21-year-long data set, moderate intensity
535 ($0.5 < \text{TOMS-AAI} < 1.0$) and high intensity ($\text{TOMS-AAI} \geq$
536 1.0) contributions of Saharan-based dust outbreaks consti-
537 tuted 18% and 3% of events, respectively. They predomi-
538 nantly took place from mid-March to the end of August
539 with the most intensive events observed in April–May. The
540 rest, with $\text{TOMS-AAI} \leq 0.5$, generally corresponded to
541 negligible dust loads observed during the entire autumn-
542 winter period, as well as a few isolated low level transports
543 undetected by TOMS.

544 [27] Comparison of TOMS-retrieved AOT with its
545 ground-based measurements suggests that the AOT can be
546 estimated by TOMS reasonably well by a factor of 0.86.
547 This value lies within the range of estimates at different
548 oceanic and land sites by *Torres et al.* [2002].

549 [28] Our findings, when complemented with those of
550 *Kubilay et al.* [2000], indicate that dust transport and
551 deposition constitute a large fraction of annual dust depo-
552 sition into the eastern Mediterranean. *Rutten et al.* [2000]
553 have already noted a positive correlation between dust and
554 surface chlorophyll concentrations and sediment trap data
555 from a 3-year-long time series at $\sim 34^\circ\text{N}$, 20°E . Thus TOMS
556 aerosol data can be used to estimate regional dust transport

and deposition, as recently provided for the Atlantic Ocean
557 by *Kaufman et al.* [2005] using the Terra-MODIS products.
558 This approach allows quantification of seasonally and
559 regionally varying inputs of dust associated biologically
560 available iron and phosphate flux into the sea.
561

[29] **Acknowledgments.** The authors would like to thank Brent
562 Holben (NASA-GSFC) for providing us with the Sun photometer within
563 the framework of the AERONET program, the NASA/GSFC/TOMS group
564 for the use of TOMS-AAI data, and Emin Özsoy for making available the
565 ECMWF trajectory analysis through collaboration with the Turkish State
566 Meteorological Office. Finally, we appreciate the constructive remarks by
567 the reviewers. This research was partly supported by the Middle East
568 Technical University Research Funding AFP-2001-07-01-01, and the
569 NATO Linkage Grant EST.CLG.977811.
570

References

- 571
572 Alpert, P., and E. Ganor (2001), Sahara mineral dust measurements from
573 TOMS; Comparison to surface observations over the Middle East for the
574 extreme dust storm, March 14–17, 1998, *J. Geophys. Res.*, *106*, 18,275–
575 18,286.
576 Alpert, P., P. Kishcha, A. Shtivelman, S. O. Krichak, and J. H. Joseph
577 (2004), Vertical distribution of Saharan dust based on 2.5-year model
578 predictions, *Atmos. Res.*, *70*, 109–130.
579 Barnaba, F., and G. P. Gobbi (2004), Aerosol seasonal variability over the
580 Mediterranean region and relative impact of maritime, continental and
581 Saharan dust particles over the basin from MODIS data in the year 2001,
582 *Atmos. Chem. Phys. Discuss.*, *4*, 4285–4337.
583 Chiapello, I., and C. Moulin (2002), TOMS and METEOSAT satellite
584 records of the variability of Saharan dust transport over the Atlantic
585 during the last two decades (1979–1997), *Geophys. Res. Lett.*, *29*(8),
586 1176, doi:10.1029/2001GL013767.
587 Chiapello, I., J. M. Prospero, J. R. Herman, and N. C. Hsu (1999), Detec-
588 tion of mineral dust over the North Atlantic Ocean and Africa with
589 Nimbus 7 TOMS, *J. Geophys. Res.*, *104*, 9277–9291.
590 Dayan, U., J. Heffter, J. Miller, and G. Gutman (1991), Dust intrusion
591 events into the Mediterranean basin, *J. Appl. Meteorol.*, *30*, 1185–1199.
592 Ganor, E. (1994), The frequency of Saharan dust episodes over Tel Aviv,
593 Israel, *Atmos. Environ.*, *28*, 2867–2871.
594 Guieu, C., Y. Bozec, S. Blain, C. Ridame, G. Sarthou, and N. Leblond
595 (2002a), Impact of high Saharan dust inputs on the dissolved iron con-
596 centrations in the Mediterranean Sea, *Geophys. Res. Lett.*, *29*(19), 1911,
597 doi:10.1029/2001GL014454.
598 Guieu, C., M.-D. Loÿe-Pilot, C. Ridame, and C. Thomas (2002b), Chemical
599 characterization of the Saharan dust end-member: Some biogeochemical
600 implications for the western Mediterranean Sea, *J. Geophys. Res.*,
601 *107*(D15), 4258, doi:10.1029/2001JD000582.
602 Hamonou, E., P. Chazette, D. Balis, F. Dulac, X. Schneider, E. Galani,
603 G. Ancellet, and A. Papayannis (1999), Characterization of the vertical
604 structure of Saharan dust export to the Mediterranean basin, *J. Geo-
605 phys. Res.*, *104*, 22,257–22,270.
606 Herman, J. R., P. K. Bhartia, O. Torres, C. Hsu, C. Seftor, and E. Celarier
607 (1997), Global distribution of UV-absorbing aerosols from Nimbus 7/
608 TOMS data, *J. Geophys. Res.*, *102*, 16,911–16,922.
609 Hsu, N. C., J. R. Herman, O. Torres, B. N. Holben, D. Tanré, T. F. Eck,
610 A. Smirnov, B. Chatenet, and F. Lavenue (1999), Comparisons of the
611 TOMS aerosol index with sun-photometer aerosol optical thickness:
612 Results and applications, *J. Geophys. Res.*, *104*, 6269–6279.
613 Israelevich, P. L., Z. Levin, J. H. Joseph, and E. Ganor (2002), Desert
614 aerosol transport in the Mediterranean regions as inferred from the TOMS
615 aerosol index, *J. Geophys. Res.*, *107*(D21), 4572, doi:10.1029/
616 2001JD002011.
617 Kaufman, Y. J., I. Koren, L. A. Remer, D. Tanré, P. Ginoux, and S. Fan
618 (2005), Dust transport and deposition observed from the Terra-Moderate
619 Resolution Imaging Spectroradiometer (MODIS) spacecraft over the
620 Atlantic Ocean, *J. Geophys. Res.*, doi:10.1029/2003JD004436, in
621 press.
622 Koçak, M., M. Nimmo, N. Kubilay, and B. Herut (2004), Spatio-temporal
623 aerosol trace metal concentrations and sources in the Levantine basin of
624 the eastern Mediterranean, *Atmos. Environ.*, *38*, 2133–2144.
625 Krom, M. D., B. Herut, and R. F. C. Mantoura (2004), Nutrient budget for
626 the eastern Mediterranean: Implications for phosphorus limitation, *Lim-
627 nol. Oceanogr.*, *49*(5), 1582–1592.
628 Kubilay, N., and C. Saydam (1995), Trace elements in atmospheric parti-
629 culates over the eastern Mediterranean: Concentrations, sources and tem-
630 poral variability, *Atmos. Environ.*, *29*, 2289–2300.
630

- 631 Kubilay, N., S. Nickovic, C. Moulin, and F. Dulac (2000), An illustration of
632 the transport and deposition of mineral dust onto the eastern Mediterranean,
633 *Atmos. Environ.*, *34*, 1293–1303.
- 634 Kubilay, N., T. Cokacar, and T. Oguz (2003), Optical properties of mineral
635 dust outbreaks over the northeastern Mediterranean, *J. Geophys. Res.*,
636 *108*(D21), 4666, doi:10.1029/2003JD003798.
- 637 Markaki, Z., K. Oikonomou, M. Kocak, G. Kouvarakis, A. Chaniotaki,
638 N. Kubilay, and N. Mihalopoulos (2003), Atmospheric deposition of
639 inorganic phosphorus in the Levantine Basin, eastern Mediterranean:
640 Spatial and temporal variability and its role in seawater productivity,
641 *Limnol. Oceanogr.*, *48*(4), 1557–1568.
- 642 Moulin, C., and I. Chiapello (2004), Evidence of the control of summer
643 atmospheric transport of African dust over the Atlantic by Sahel sources
644 from TOMS satellites (1979–2000), *Geophys. Res. Lett.*, *31*, L02107,
645 doi:10.1029/2003GL018931.
- 646 Moulin, C., C. E. Lambert, F. Dulac, and U. Dayan (1997), Control of
647 atmospheric export of dust from North Africa by the North Atlantic
648 Oscillation, *Nature*, *387*, 691–694.
- 649 Moulin, C., et al. (1998), Satellite climatology of African dust transport in
650 the Mediterranean atmosphere, *J. Geophys. Res.*, *103*, 13,137–13,144.
- 651 Özsoy, E., N. Kubilay, S. Nickovic, and C. Moulin (2001), A hemispheric
652 dust storm affecting the Atlantic and Mediterranean in April 1994: Ana-
653 lyses, modeling, ground-based measurements and satellite observations,
654 *J. Geophys. Res.*, *106*, 18,439–18,460.
- 655 Prospero, J. M., P. Ginoux, O. Torres, S. Nicholson, and T. Gill (2002),
656 Environmental characterization of global sources of atmospheric soil dust
657 identified with the Nimbus 7 Total Ozone Mapping Spectrometer
658 (TOMS) absorbing aerosol product, *Rev. Geophys.*, *40*, 1–31.
- 659 Ridame, C., and C. Guieu (2002), Saharan input of phosphate to the oligo-
660 trophic water of the open western Mediterranean Sea, *Limnol. Oceanogr.*,
661 *47*(3), 856–869.
- Rutten, A., G. J. de Lange, P. Ziveri, J. Thomson, P. J. M. van Santvoort, 662
S. Colley, and C. Corselli (2000), Recent terrestrial and carbonate 663
fluxes in the pelagic eastern Mediterranean: A comparison between 664
sediment trap and surface sediment, *Palaeogeogr. Palaeoclimatol.* 665
Palaeoecol., *158*, 197–213.
- Torres, O., P. K. Bhartia, J. R. Herman, Z. Ahmad, and J. Gleason (1998), 667
Derivation of aerosol properties from satellite measurements of backscat- 668
tered ultraviolet radiation: Theoretical basis, *J. Geophys. Res.*, *103*, 669
17,099–17,110.
- Torres, O., P. K. Bhartia, J. R. Herman, A. Sinyuk, P. Ginoux, and 671
B. Holben (2002), A long-term record of aerosol optical depth 672
from TOMS observations and comparison to AERONET measure- 673
ments, *J. Atmos. Sci.*, *59*, 398–413.
- Torres, O., P. K. Bhartia, A. Sinyuk, E. J. Welton, and B. Holben (2005), 675
Total Ozone Mapping Spectrometer measurements of aerosol absorption 676
from space: Comparison to SAFARI 2000 ground-based observations, 677
J. Geophys. Res., doi:10.1029/2004JD004611, in press. 678
- Washington, R., M. Todd, N. J. Middleton, and A. Goudie (2003), Dust- 679
storm source areas determined by the total ozone monitoring spectro- 680
meter and surface observations, *Ann. Assoc. Am. Geogr.*, *93*(2), 297–313. 681
- M. Koçak, N. Kubilay, and T. Oguz, Institute of Marine Sciences, Middle 683
East Technical University, ODTU-DBE, P.K. 28 Erdemli 33731, Turkey. 684
(mustafa@ims.metu.edu.tr; kubilay@ims.metu.edu.tr; oguz@ims.metu. 685
edu.tr) 686
- O. Torres, Joint Center for Earth Systems Technology, University of 687
Maryland, Baltimore County, Baltimore, MD, USA. (torres@qhearts.gsfc. 688
nasa.gov) 689

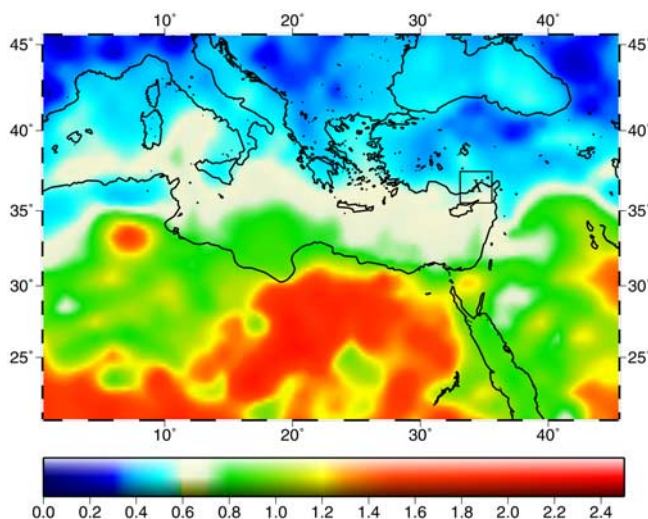


Figure 1. April-mean TOMS-AAI distribution obtained by averaging 21 years of daily data at each pixel of the analysis region. Three distinct regions with different TOMS-AAI properties are clearly indicated in the map. North Africa (red) identifies the major dust load (TOMS-AAI ≥ 1.0), whereas Southern Europe and Asia Minor (blue) (TOMS-AAI ≤ 0.4) represent a negligible dust load. The eastern Mediterranean is a transitional region with latitudinal TOMS-AAI variations between 1.0 in the south and 0.5 in the north. The Erdemli sampling station, as well as a small box around it, near the northeastern corner of the eastern Mediterranean is also shown in the figure.

690

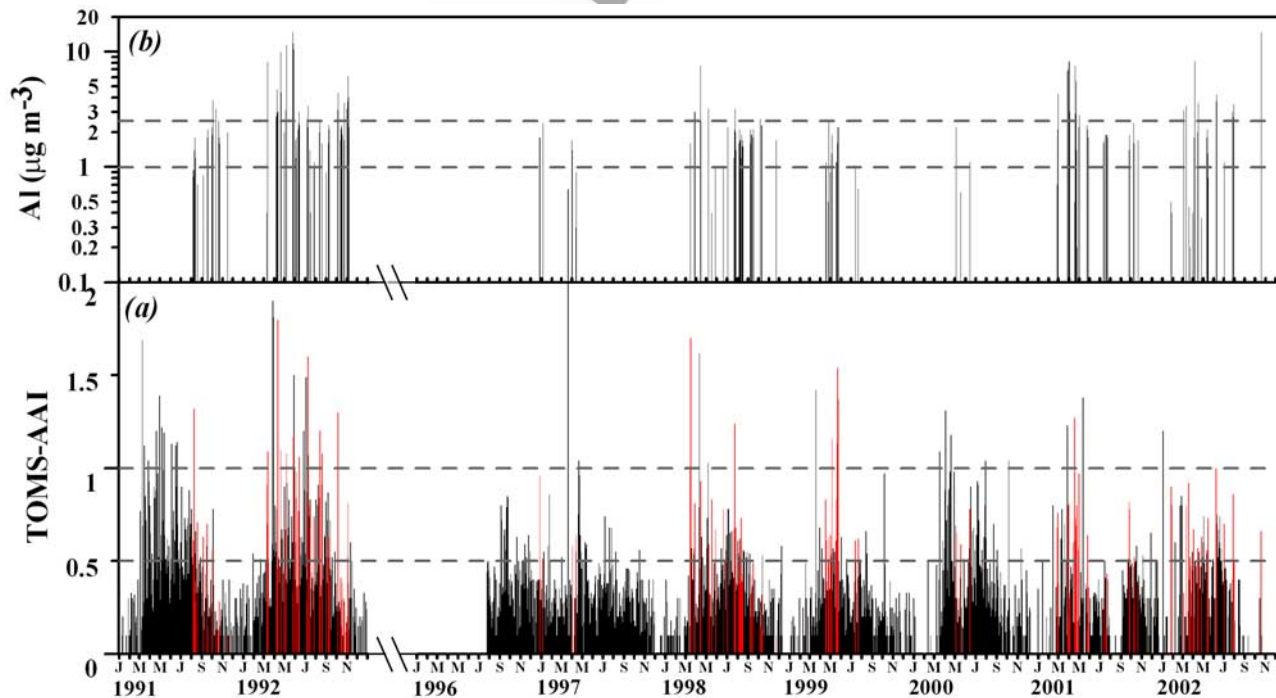


Figure 2. (a) Daily TOMS-AAI distribution around Erdemli during 9-year period from 1 January 1991 to 31 December 1992 and 26 July 1996 to 31 December 2002 (black bars). Superimposed on this data, red bars indicate dust events either with TOMS-AAI > 0.5 or aerosol Al > 1.0 or both, for common days with TOMS-AAI and aerosol Al data. Two broken horizontal lines represent the threshold AAI values for moderate and intense dust events classified on the basis of TOMS retrievals. (b) Daily aerosol Al ($\mu\text{g m}^{-3}$) measurements performed during the study period. The data represent a subset of all the available measurements corresponding to the events shown by red bars in Figure 2a. Two broken horizontal lines indicate the threshold values for moderate and intense dust events classified according to the ground-based measurements.

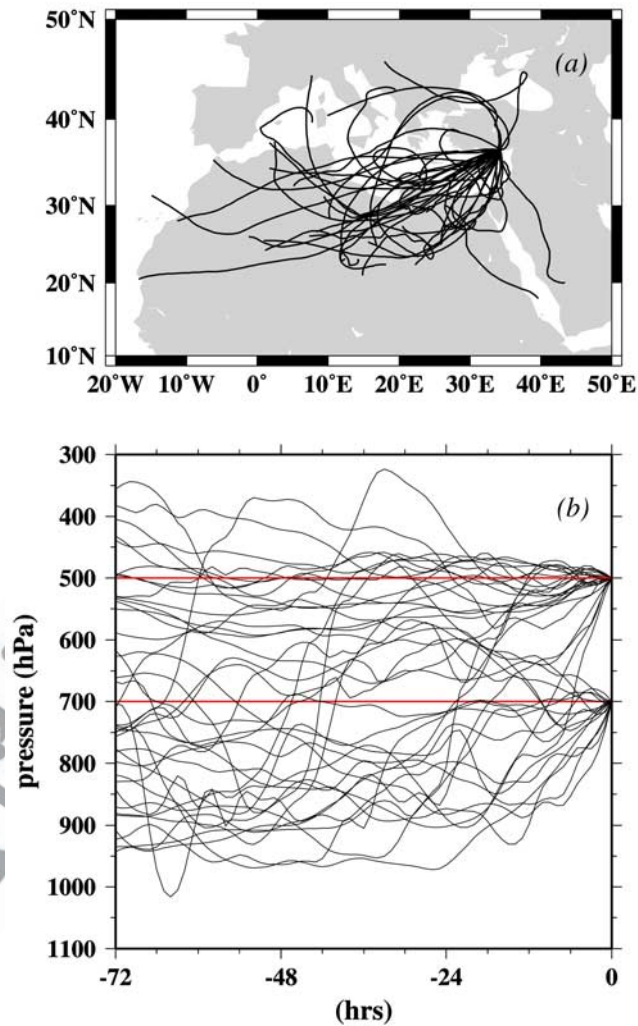


Figure 4. (a) Three-day back trajectories for high altitude transport events arriving at 700- and 500-hPa pressure levels to Erdemli, and (b) their vertical motions along the trajectories. They represent some selected events out of a total 67 during 1991–1992 and 1996–2002.

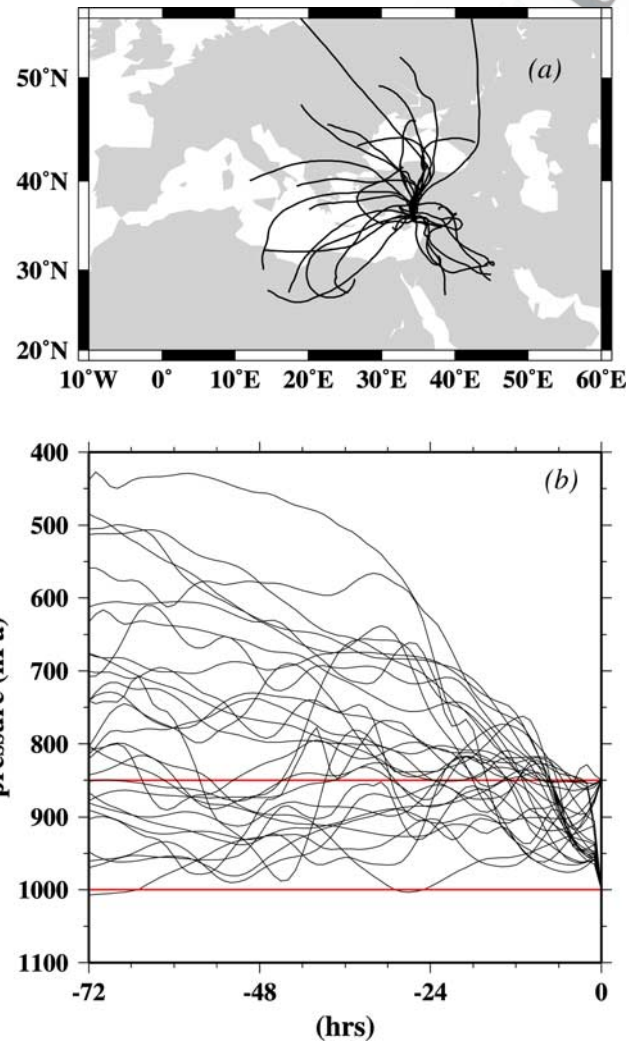


Figure 5. (a) Three-day back trajectories for low altitude transport events arriving at 1000- and 850-hPa pressure levels to Erdemli, and (b) their vertical motions along the trajectories. They represent some selected events out of a total 31 during 1991–1992 and 1996–2002.